MicroRNAs as Key Regulators of Plant Flowering Time Adaptation to Climate Change

Qiong A. Liu [1], Kun Zhang [2, 3], Erkang Wang [2, 3], Jin Wang[4]

[1] IvyGen LLC, Cranbury, NJ 08512. alisonliu333@outlook.com

[2] School of Applied Chemistry and Engineering, University of Science and Technology of China, China.

[3] State Key Laboratory of Electroanalytical Chemistry, Changchun Institute of Applied Chemistry, Chinese Academy of Sciences, China.

[4] Department of Chemistry and of Physics, Stony Brook University, NY 11794

Introduction:

Flowering is crucial for plant reproduction, biomass, and seed production, with its timing synchronized to developmental stages, weather conditions, and pollinator availability. Disruptions to flowering time can negatively impact plant productivity, species survival, and ecosystem stability. While elevated CO_2 and rising temperatures are known to impact flowering time, the underlying mechanisms remain unclear.

- MicroRNAs (miRNAs) play a key role in regulating gene expression and are highly responsive to environmental changes. Using next-generation sequencings, we identified miRNA-regulated pathways affected by doubled atmospheric CO_2 or a 3–6°C temperature increase. The miR156/157-regulated transcriptional network emerged as central to early flowering induced by elevated CO_2 [1].
- We further investigated, using the global landscape of network dynamics analysis, the robustness of the miR156/157 network in response to varying CO_2 levels and its impact on flowering time [2]. Our analysis showed that CO_2 concentrations of 200–300 ppm dramatically advanced flowering time, while 400–800 ppm had a mild effect. We confirmed the buffering role of feedback regulation, identified an inverse relationship between flowering time and its variance, and highlighted sensitive features within the network.
- Our research provides the first physical basis for plant species, uncovering novel regulatory mechanisms and the resilience of miRNA networks to increasing CO_2, thereby influencing flowering time and offering a promising strategy for enhancing plant adaptation and resilience to climate change.

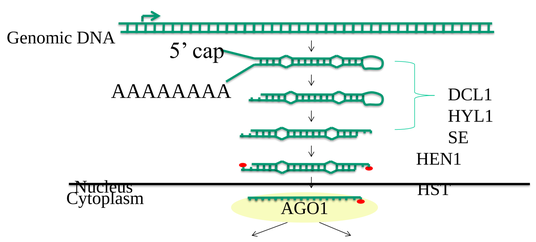

Figure 1. Mechanism of miRNA biogenesis and their role in inhibiting gene expression in *Arabidopsis* plants.
Primary miRNA (pri-miRNAs) are transcribed from genome, and then processed into precursor miRNAs (pre-miRNA), followed by cleavage of loop region of hairpin to form miRNA–miRNA* duplexes. These processes are mediated by coordinated activities of DCL1, HYL1 and SE within the nucleus. The top strand of miRNA–miRNA* duplexes is miRNA, while the bottom one is miRNA*. Both strands are 2′-*O*-methylated on the 3′-terminal ribose by HEN1, a small RNA methyltransferase (2′-*O*-methyl groups are indicated by red dots). The miRNA strand is incorporated into an AGO1-containing RNA-induced silencing complex (miRISC), which mediate either mRNA cleavage or translational inhibition. miRISCs or an intermediate is exported from the nucleus to the cytoplasm by the exportin-5 homolog HASTY (HST).

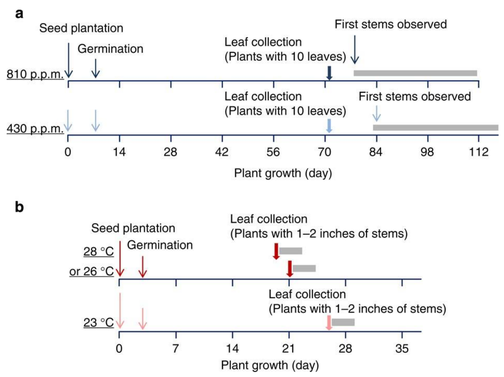

Figure 2: Elevated CO_2 and temperature result in early plant flowering

Presented are *Arabidopsis* plant growing periods starting from seed plantation to flowering time under (a) 430 and 810 ppm [CO_2] and (b) 23 °C and 26 °C or 28 °C temperatures. Big arrows indicate the time when leaf samples were collected. Uppermost fully expanded leaves were collected from 10 leaves stage *Arabidopsis* plants grown under different CO_2 concentrations before bolting stage or from plants with 1–2 inches of stems grown under different temperatures at the early bolting stage. Dark blue: 810 ppm; light blue: 430 ppm; red: 26 °C or 28 °C; pink: 23 °C; grey rectangles: the period of time when plant flowering onset.

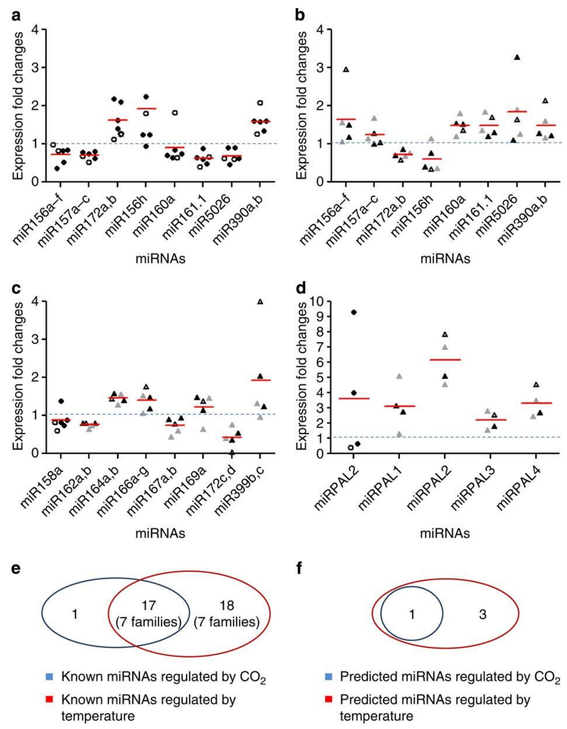

Figure 3: MiRNAs differentially regulated by elevated CO_2 and temperatures.
MiRNA fold changes were calculated by 810 ppm- over 430 ppm-, 28 °C-over 22 °C- or 23 °C-, or 26 °C-over 23 °C-treated samples. The overlapping oval shapes indicate the numbers of miRNAs that were regulated by (e) temperatures and (f), CO_2 conditions.

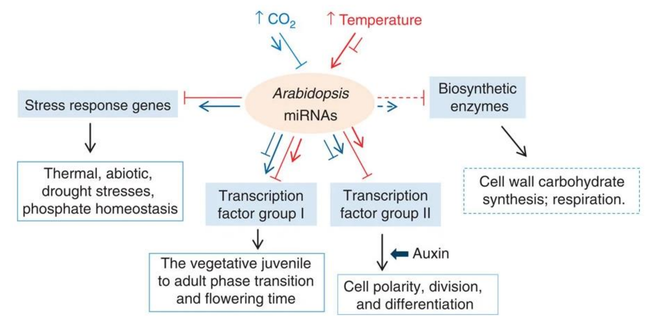

Figure 4: Differentially expressed miRNAs in regulation of development. The effects of elevated [CO_2] and elevated temperature on miRNAs, the target genes of miRNAs, and their biological functions. Red color, temperature regulated; blue color, CO_2 regulated. ↑: upregulation; T, downregulation. The length of ↑ or T represents the relative numbers of miRNAs. The dash lines and boxes indicate the predicted results. The boxes with blue background contain miRNA target genes. Inside boxes with the blue outline are annotated functions of miRNA targets. The large black arrow indicates the auxin mediated.

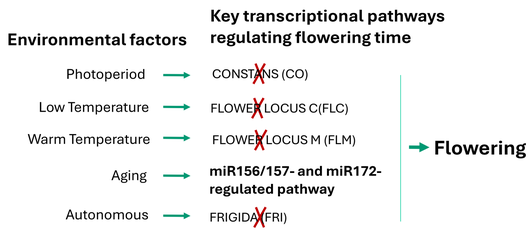

Figure 5: 800 ppm [CO_2] specifically affects miR156/157-regulated flowering time pathway.

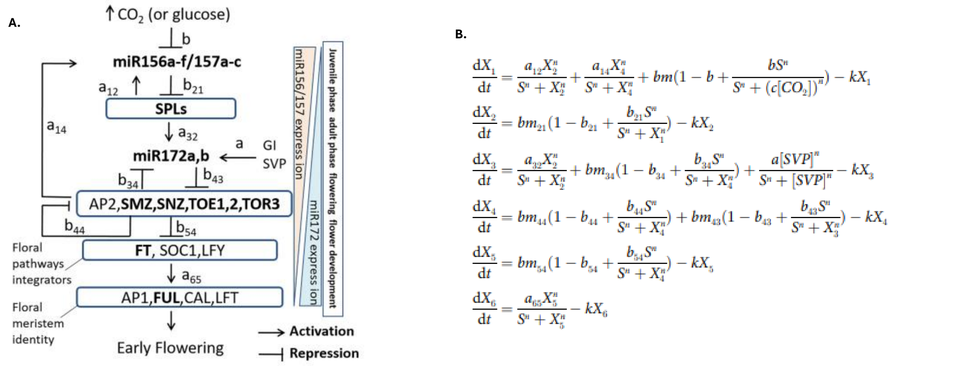

$$\frac{dX_1}{dt} = \frac{a_{12}X_2^n}{S^n + X_2^n} + \frac{a_{14}X_4^n}{S^n + X_4^n} + bm(1 - b + \frac{bS^n}{S^n + (c[CO_2])^n}) - kX_1$$

$$\frac{dX_2}{dt} = bm_{21}(1 - b_{21} + \frac{b_{21}S^n}{S^n + X_1^n}) - kX_2$$

$$\frac{dX_3}{dt} = \frac{a_{32}X_2^n}{S^n + X_2^n} + bm_{34}(1 - b_{34} + \frac{b_{34}S^n}{S^n + X_4^n}) + \frac{a[SVP]^n}{S^n + [SVP]^n} - kX_3$$

$$\frac{dX_4}{dt} = bm_{44}(1 - b_{44} + \frac{b_{44}S^n}{S^n + X_4^n}) + bm_{43}(1 - b_{43} + \frac{b_{43}S^n}{S^n + X_3^n}) - kX_4$$

$$\frac{dX_5}{dt} = bm_{54}(1 - b_{54} + \frac{b_{54}S^n}{S^n + X_4^n}) - kX_5$$

$$\frac{dX_6}{dt} = \frac{a_{65}X_5^n}{S^n + X_5^n} - kX_6$$

Figure 6: Modeling of the effects of elevated [CO_2] (or glucose) on the miR156/157-regulated flowering time network

A. miR156/157-regulated flowering time network. Bold highlights genes whose expressions can be affected by elevated [CO_2]. The relationship between CO_2 and glucose is represented by the photosynthesis reaction: $6CO_2 + 6H_2O \rightarrow C_6H_{12}O_6 + 6O_2$.

B. A set of six ordinary differential equations. Gene regulatory models were constructed to represent the dynamics of the miR156/157 network. X_i (i = 1, 2…6) represents the expression of miR156/157, SPL family, miR172, AP2 family, FT, and AP1 family. a_{ij} and b_{ij} are the activation and repression strength parameter from gene *j* to gene *I*, respectively. bm_{ij} is the maximum repression rate from gene j to gene i. k is the degradation rate constant. *n* is Hill coefficient. *S* is the Hill constant, or the threshold representing by the half-maximum effective concentration values.

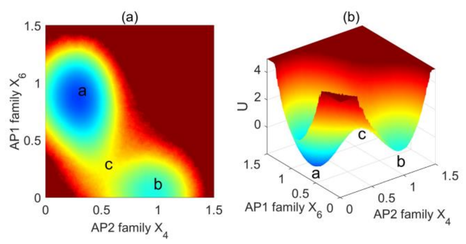

Figure 7: Identification of two steady states in the network landscape, the juvenile state and the flowering state.

(a) The two-dimensional landscape of the flowering network.

(b) The three-dimensional landscape of the flowering network. (The state "a" denotes the flowering state; the state "b" denotes the juvenile state; the state "c" is the saddle point of the landscape).

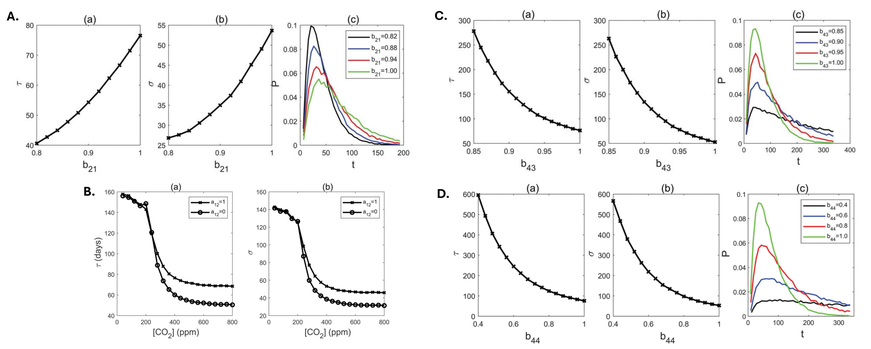

Figure 8. Flowering times and their variances are inversely related

A. (a) Mean first passage time (MFPT, Unit: days), (b) Standard deviation (SD), and (c) the distribution of first passage time (FPT) with different parameter b21.

B. (a) MFPT, and (b) SD with different [CO_2] after removing a_{12}, the feedback regulation of SPLs to miR156/157.

C. (a) MFPT, (b) SD, and (c) the distribution of FPT with different parameter b_{43}.

D. (a) MFPT, (b) SD, and (c) the distribution of FPT with different parameter b_{44}.

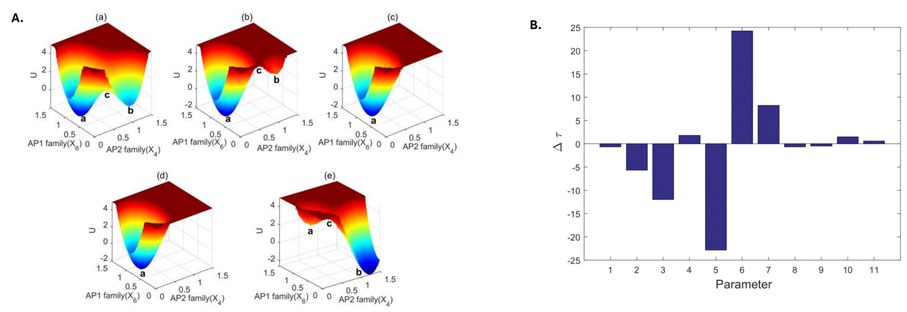

Fig 9: All feedback regulations essential, with miR172-AP2 loop being the most sensitive

A. The landscapes of the flowering network after removing different feedback regulations. (a) the normal condition; (b) removing the SPLs positive feedback regulation of miR156 (a_{12} = 0); (c) removing the AP2 family positive regulation of miR156 (a_{14} = 0); (d) removing the AP2 family negative regulation of miR172 (b_{34} = 0); (e) removing the AP2 family self-suppression (b_{44} = 0).

B. Global sensitivity analysis in terms of the MFPT. (Negative values mean accelerated flowering time.) (Parameter: 1. a_{12}; 2. a_{14}; 3. b_{21}; 4. a_{32}; 5. b_{34}; 6. b_{43}; 7. b_{44}; 8. b_{54}; 9. a_{65}; 10. [CO_2]; 11. [SVP]).

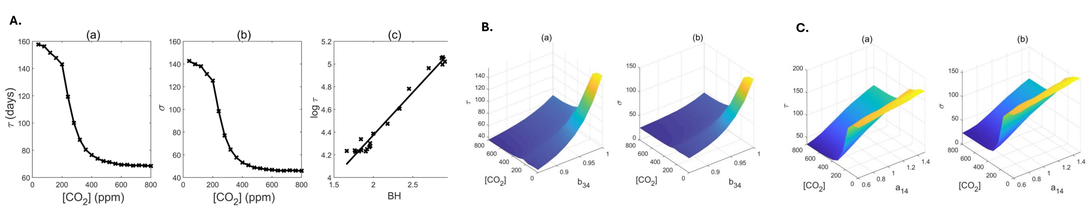

Figure 10: Raising CO_2 from 200 to 400 ppm sharply accelerates flowering, with much reduced impact between 400 and 800 ppm.

A. (a) Mean first passage time (MFPT, Unit: days) with different [CO_2] (Unit: ppm). (b) Standard deviation with different [CO_2]. (c) Logarithm of MFPT versus barrier height (BH = Uc-Ub) in different [CO_2].

B. (a) Mean first passage time with different parameters b_{34} and [CO_2] (b) Standard deviation with different parameter b_{34} and [CO_2].

C (a) Mean first passage time with different parameter a_{14} and [CO_2] (b) Standard deviation with different parameter a_{14} and [CO_2].

Conclusions:

- The onset of early flowering induced by elevated atmospheric CO_2 (400 to 800ppm) is mediated by the miR156/157- and miR172-regulated transcriptional network.
- CO_2 concentration of 400–800ppm mildly advance flowering time, in contrast to the dramatic changes observed from 200 to 300ppm.
- The feedback regulation of miR156 by SPLs plays a key role in mitigating the impact of increasing CO_2 on flowering time.
- A correlation between delayed flowering time and increased variance suggests an intrinsic network adaptation mechanism.
- The miR172 regulation of AP2s and its feedback loop are the most sensitive features in this network.
- All feedback regulations are essential for maintaining both juvenile and adult states, as well as the transition timing between them.
- Our research provides the first physical basis for plant species, aiding in the elucidation of novel regulatory mechanisms and the robustness of the miRNAs-regulated network in response to increasing CO_2, therefore influencing flowering time. This study also provides a promising strategy for engineering plant flowering time to improve adaptation and resilience.

Acknowledgements:

The sequencing work was supported by Brookhaven National Lab Research Direction fund to Qiong Liu and NSF EAGER award (Award #: 1036043) to Qiong Liu and Michael Zhang. The *Arabidopsis* plants were grown at Yale University and Oak Ridge National Lab.

References:

1. May P, Liao W, Wu Y, Shuai B, McCombie WR, Zhang MQ, **Liu QA*.** (2013) Nat Commun. 4: 2145
Zhang K, Wang E, **Liu QA***, Wang J*. (2023) PLoS Comput Biol. 19(12): e1011738.